Catalysis Today 142 (2009) 70–77

Contents lists available at ScienceDirect

Catalysis Today

journal homepage: www.elsevier.com/locate/cattod

Fischer–Tropsch synthesis over un-promoted and Re-promoted γ-Al_2O_3 supported cobalt catalysts with different pore sizes

Øyvind Borg [a,1], Nina Hammer [a,1], Sigrid Eri [b], Odd Asbjørn Lindvåg [c], Rune Myrstad [c], Edd A. Blekkan [a], Magnus Rønning [a], Erling Rytter [a,b], Anders Holmen [a,*]

[a] Department of Chemical Engineering, Norwegian University of Science and Technology, NO-7491 Trondheim, Norway
[b] StatoilHydro R&D, Research Centre, Postuttak, NO-7005 Trondheim, Norway
[c] SINTEF Materials and Chemistry, NO-7465 Trondheim, Norway

ARTICLE INFO

Article history:
Available online 11 February 2009

Keywords:
Fischer–Tropsch synthesis
Cobalt
Rhenium
Alumina
Pore size
Cobalt-time yield
Site-time yield
C_{5+} selectivity

ABSTRACT

The effect of rhenium on the Fischer–Tropsch synthesis activity and selectivity of γ-Al_2O_3 supported cobalt catalysts was investigated in fixed-bed reactors at T = 483 K, P = 20 bar, and H_2/CO = 2.0. Catalysts containing 20 wt.% cobalt and 0 or 0.5 wt.% rhenium were prepared by incipient wetness impregnation of different γ-Al_2O_3 supports with aqueous solutions of cobalt nitrate hexahydrate and for the Re-promoted catalysts, also perrhenic acid. The γ-Al_2O_3 supports had very different pore characteristics. The post-calcination Co_3O_4 crystallite size was predominantly controlled by the γ-Al_2O_3 support pore diameter. Presence of Re had only a minor effect on the crystallite size. For all catalysts, supported Co_3O_4 was reduced in two steps to Co^0 with CoO as intermediate species. However, while reduction of Co_3O_4 to CoO took place in the same temperature range for all catalysts, the reduction temperature of CoO to Co^0 was dependent on the catalyst properties. Large particles present in wide pores were easier to reduce than small particles located in narrow pores. In addition, Re promoted the reduction of CoO. The effect of rhenium as a reduction promoter was less pronounced at increasing pore size and particle size. Re also had a similar positive impact on the cobalt dispersion of the catalysts. Although Re significantly increased the Fischer–Tropsch synthesis cobalt-time yield, it did not modify the site-time yield. The deactivation rates of all the catalysts were also similar up to 100 h on stream. Positive correlations were found between the catalyst pore diameter and the C_{5+} selectivity and between the cobalt particle size and the C_{5+} selectivity. Re had a consistent positive, albeit small, effect on the C_{5+} selectivity.

1. Introduction

Cobalt is favoured for the synthesis of long-chain hydrocarbons from natural gas-based synthesis gas because of its high activity, high selectivity to linear paraffins, high resistance towards deactivation, and low water–gas shift activity. In order to maximise the exposure of cobalt to gaseous reactants, the metal is normally dispersed on a high surface area support. In some cases, the support interacts strongly with the active phase. Metal–support interactions may leave a fraction of the cobalt chemically inactive after reduction. In order to reduce the amount of non-reduced cobalt, a small amount of a second metal can be introduced into the catalyst system. Rhenium is a frequent choice as reduction promoter. The first application of rhenium in combination with cobalt for Fischer–Tropsch synthesis was reported in 1986 by Mauldin [1]. It is generally accepted that rhenium mainly catalyses the reduction of cobalt species interacting with the support. Hilmen et al. [2] concluded that rhenium promotes reduction by hydrogen spillover, and that no direct contact between cobalt and rhenium is necessary in order to obtain the promoting effect.

Although the Fischer–Tropsch activity usually increases when Re is present, the increase can often be proportionally correlated with the increase in cobalt dispersion. Thus, the site-time yield is constant [3–6]. While it is well known that Re facilitates the reduction of cobalt oxide, the effect of Re on the product selectivity is not equally clear. Bertole et al. [5] concluded from steady-state isotopic transient kinetics analysis that Re, at a Re/Co weight ratio of 0.1, does not influence the Fischer–Tropsch selectivity. Similar results have been found by others [3,4]. On the other hand, Schanke et al. [7] observed that Re increased the selectivity to long-chain hydrocarbons for cobalt supported on low (15 m^2/g) and high surface area (190 m^2/g) alumina. Storsæter et al. [6] investigated the Fischer–Tropsch synthesis behaviour of un-promoted and Re-promoted

* Corresponding author. Tel.: +47 73 59 41 51; fax: +47 73 59 50 47.
E-mail address: anders.holmen@chemeng.ntnu.no (A. Holmen).
[1] Present address: StatoilHydro R&D, Research Centre, Postuttak, NO-7005 Trondheim, Norway.

0920-5861/$ – see front matter © 2009 Elsevier B.V. All rights reserved.
doi:10.1016/j.cattod.2009.01.012

cobalt on γ-Al_2O_3, SiO_2, and TiO_2. Presence of Re increased the C_{5+} selectivity of the SiO_2 and TiO_2-based samples.

To summarise, although the effect of Re on the activity is well established, the effect of Re on the product selectivity is not as clear. As Bertole et al. [5] timely pointed out, the product selectivity is very sensitive to reaction conditions, conversion level, and possible mass transfer limitations. Accordingly, without strict control of reaction conditions, it is impossible to establish the effect of Re on the product selectivity. Also, since the differences in C_{5+} selectivity between un-promoted and promoted cobalt catalysts are relatively small [3–7], it is challenging to separate real effects from experimental errors. For these reasons, the purpose of the present study was to investigate experimentally the effect of Re in a systematic approach. The metal precursors were added to γ-Al_2O_3 supports using exactly the same preparation method and amount of active components. Also, the product selectivity of all the catalysts was compared at the same CO conversion level.

2. Experimental

2.1. Catalyst preparation

Supported catalysts containing 20 wt.% cobalt and 0 or 0.5 wt.% rhenium were prepared by one-step incipient wetness co-impregnation of different γ-Al_2O_3 supports (Sasol GmbH Puralox series) with aqueous solutions of cobalt nitrate hexahydrate and for the Re-promoted catalysts, also perrhenic acid. The supports and aqueous metal solutions were mixed under ambient temperature and pressure conditions. Before impregnation, the supports (53–90 μm) were calcined under air (0.2 L/(g h)) in a fixed-bed quartz reactor at 773 K for 10 h. The bed thicknesses were approximately 5 cm. A rate of 1 K/min was used to heat the samples from ambient temperature to 773 K. All supports were low in sodium (<30 ppm), an element which has a very negative effect on the Fischer–Tropsch synthesis activity [8,9].

After impregnation, the catalysts were dried in a stationary oven kept at 393 K for 3 h. To ensure homogeneity, the samples were stirred gently every 15 min the first hour and every 30 min the last 2 h. The catalysts were then calcined at 573 K for 16 h in the same equipment as used for the support calcination. The flow rates and bed thicknesses were also identical. However, the temperature was increased by 2 K/min from ambient temperature to 573 K. Finally, the catalysts were sieved and the 53–90 μm fractions collected. Further pre-treatment was done *in situ*.

The supports were named according to their pore sizes: "NPA" (narrow pore alumina), "MPA" (medium pore alumina), and "WPA" (wide pore alumina) as shown in Table 1. After cobalt impregnation, the catalyst nomenclature was "Co/NPA", "Co/MPA", and "Co/WPA". Finally, after cobalt and rhenium impregnation, the names were "CoRe/NPA", "CoRe/MPA", and "CoRe/WPA".

While the promoted catalysts have been prepared and described previously [9], the un-promoted catalysts have been prepared exclusively for this investigation.

Table 1
Nitrogen sorption data for the γ-Al_2O_3 supports and the impregnated samples. For the nitrogen sorption data, the experimental error ($\pm 2\sigma$) is ± 10 m^2/g for the surface areas, ±0.5 nm for the average pore diameters, and ± 0.02 cm^3/g for the pore volumes. The uncertainty is based on three independent runs of all the samples.

Sample	BET surface area (m^2/g)	Average pore diameter (nm)	Pore volume (cm^3/g)
NPA	184	7.4	0.48
Co/NPA	141	6.8	0.31
CoRe/NPA	143	7.1	0.30
MPA	186	12.3	0.73
Co/MPA	138	11.5	0.49
CoRe/MPA	148	11.6	0.50
WPA	114	26.7	0.86
Co/WPA	77	26.6	0.58
CoRe/WPA	92	23.7	0.57

2.2. Support and catalyst characterization

2.2.1. Nitrogen adsorption/desorption

Nitrogen adsorption–desorption isotherms were measured on a Micromeritics TriStar 3000 instrument, and the data were collected at 77 K. The samples (0.3 g, 53–90 μm) were outgassed at 573 K overnight prior to measurement.

The surface area was calculated from the Brunauer–Emmett–Teller (BET) equation [10], while the total pore volume and pore size distribution were found applying the Barrett–Joyner–Halenda (BJH) method [11]. The nitrogen desorption branch was chosen for pore size analysis.

2.2.2. X-ray diffraction

X-ray diffraction patterns of all the supports and catalysts were recorded at ambient temperature on a Siemens D5005 X-ray diffractometer using Cu Kα radiation. The samples were crushed prior to measurement. The scans were recorded in the 2θ range between 10° and 90° using a step size of 0.04° and a step time of 15 s.

The average Co_3O_4 crystallite size was calculated from the Scherrer equation [12] using the (3 1 1) peak located at $2\theta = 36.9°$. A K factor of 0.89 was used in the Scherrer formula. In order to obtain a high signal-to-noise ratio and, consequently, minimise the experimental error, new scans were recorded only in the 2θ range between 32° and 43°. The step size was still 0.04°, but the step time was increased by a decade. Lanthanum hexaboride was used as reference material to determine the instrumental line broadening.

2.2.3. Temperature programmed reduction

Temperature programmed reduction (TPR) experiments were performed in a U-shaped tubular quartz reactor heated by an electrical furnace [13]. The calcined samples (0.2 g, 53–90 μm) were exposed to a reducing gas mixture consisting of 7% H_2 in argon while the temperature was increased at 10 K/min from ambient to 1203 K.

TPR profiles were also recorded after *in situ* reduction of the catalysts. In this case, the calcined samples (0.2 g, 53–90 μm) were reduced in a flow of pure hydrogen at 623 K. A ramp rate of 1 K/min was used to increase the temperature from ambient to 623 K. This temperature was held for 16 h before subsequently cooling the samples to 298 K. The catalysts were flushed with He for 1 h, and finally heated at a rate of 10 K/min to 1203 K in 7% H_2 in Ar.

A cold trap containing a mixture of 2-propanol and dry ice was used to eliminate water and other condensable products from the product gas mixtures. The consumption of hydrogen was obtained from the thermal conductivity difference between the reference and product gas. Calibration was done by reduction of Ag_2O powder.

2.2.4. Pulse oxidation

Pulse oxidation was performed on a Micromeritics AutoChem II 2920 unit. The catalyst samples (0.3 g, 53–90 μm) were reduced *in situ* under flowing hydrogen for 16 h at 623 K. The temperature was linearly ramped from ambient to 623 K at a rate of 1 K/min. After reduction, the samples were flushed in flowing He for 1 h and subsequently heated to 673 K at 1 K/min keeping the same gaseous atmosphere. A series of pulses of oxygen were passed through the catalyst bed at 673 K. The amount of oxygen consumed by the samples was calculated from the number of pulses reacting with

the samples and the known pulse volume. The degree of reduction was calculated assuming that all cobalt in metallic form was oxidised to Co_3O_4. Any oxidation of Re to Re_2O_7 was not considered in the calculations.

2.2.5. Hydrogen chemisorption

Hydrogen adsorption isotherms were recorded on a Micromeritics ASAP 2010 unit. The samples (0.5 g, 53–90 μm) were evacuated at 313 K for 1 h, and then reduced *in situ* in flowing hydrogen at 623 K for 16 h. The temperature was increased by 1 K/min from 313 to 623 K. After reduction, the samples were evacuated at 603 K for 1 h and for 30 min at 373 K before cooling to 313 K. The adsorption isotherm was recorded in the pressure interval ranging from 15 to 500 mmHg. The amount of chemisorbed hydrogen was determined by intrapolating the straight-line portion of the isotherm to zero pressure. Furthermore, in order to calculate the dispersion, it was assumed that two cobalt surface atoms are covered by one hydrogen molecule [14], and that rhenium does not contribute to the amount of hydrogen adsorbed.

The apparent cobalt metal particle size ($d(Co^0)_{uncorrected}$) can be calculated from the cobalt dispersion (D) by assuming spherical, uniform cobalt metal particles with site density of 14.6 at./nm^2 [15]. These assumptions give the following formula:

$$d(Co^0)_{uncorrected}\,(nm) = \frac{96}{D(\%)} \quad (1)$$

However, since the difference in reducibility of un-promoted and Re-promoted samples can be substantial, it is necessary to correct Eq. (1) for the degree of reduction (*DOR*). Thus, the corrected particle size was calculated from

$$d(Co^0)_{corrected}\,(nm) = \frac{96}{D(\%)} \times DOR \quad (2)$$

2.2.6. X-ray absorption spectroscopy (XAS)

Transmission XAS data were collected at the Swiss-Norwegian Beamlines (SNBL) at the European Synchrotron Radiation Facility (ESRF), Grenoble, France. Spectra were collected at the Co K-edge (7709 eV) using a double crystal Si(1 1 1) monochromator. Higher order harmonics were rejected by a chromium-coated mirror angled at 3.5 mrad with respect to the beam to give a cut-off energy of approximately 15 keV. The beam currents ranged from 130 to 200 mA at 6.0 GeV. A Co foil (thickness 12.5 μm) was used for energy calibration and as an internal standard during the experiments.

The amount of sample was calculated from element mass fractions and the absorption coefficients of the constituent elements 50 eV above the absorption edge to give an absorber optical thickness close to 2.0 absorption lengths. The *in situ* sample cell consists of Al (4 μm) windows and was heated by two cartridge heaters. In order to pre-heat the gases, heating tapes were wrapped around the gas-lines close to the cell inlet. The gas-lines after the reactor were also heated.

The experiments were performed in two steps. In the first step, 5% H_2/He (20 ml) was passed over the catalyst to obtain metallic cobalt. The samples were reduced at 673 K for 3.5 h. A rate of 5 K/min was used to heat the samples from room temperature to the final reduction temperature. In the second step, the reduced catalysts were exposed to diluted synthesis gas (5% ($CO + H_2$)/He (20 ml/min)). CO hydrogenation was performed at T = 483 K, P = 1 bar, and H_2/CO = 2.0. The catalysts were kept on stream for 6 h. Short scans of the edge profiles of the Co K-edge (*i.e.* XANES scans) were collected during reduction and reaction conditions.

2.2.7. XANES data analysis

The XAS data analysis program WinXAS v. 3.1 [16] was used for examining the XANES spectra. The identification of the number of phases present during *in situ* reduction was done by a principal component analysis (PCA) of the experimental spectra [17]. Reference spectra were then used in a linear combination fitting procedure to determine the quantity of each phase present. The algorithm uses a least squares procedure to refine the sum of a given number of reference spectra to an experimental spectrum.

2.3. Activity and selectivity measurements

Fischer–Tropsch synthesis was performed in four parallel fixed-bed reactors (stainless steel, 10 mm inner diameter). The samples (1.0 g, 53–90 μm) were diluted with inert silicon carbide particles (20.0 g, 75–150 μm) in order to improve the temperature distribution along the catalyst beds.

The samples were reduced *in situ* in hydrogen at 1 bar while the temperature was increased at 1 K/min to 623 K. After 16 h of reduction, the catalysts were cooled to 443 K. The system was then pressurised to 20 bar and synthesis gas of molar ratio H_2/CO = 2.0 (and 3% N_2 as internal standard) was introduced to the reactor. To avoid run-away and catalyst deactivation at start-up, the temperature was increased slowly to the reaction temperature 483 K.

Each experiment was divided into two periods which lasted for 24 and 76 h, respectively. The following conditions were used:

- Period 1: Synthesis gas at a flow rate of 250 N ml/min.
- Period 2: Synthesis gas at an adjusted flow rate to give a target CO conversion of 50%.

Heavy hydrocarbons were collected in a heated trap (363 K) and liquid products were removed in a cold trap (298 K). The effluent gaseous product was analysed on an on-line Agilent 6890 gas chromatograph equipped with a thermal conductivity detector (TCD) and a flame ionisation detector (FID). H_2, N_2, CO, CH_4, and CO_2 were separated by a Carbosieve column and analysed on the TCD. Hydrocarbon products were separated by a HP-PLOT Al_2O_3 "M" column and detected on the FID. CH_4 was used to combine the TCD and FID analyses.

Activity is reported as cobalt-time yield (mol CO/(mol(Co) s)). The C_{5+} selectivity was calculated by subtracting the amount of C_1–C_4 hydrocarbons and CO_2 in the product gas mixture from the total mass balance. When the C_{5+} selectivity is given as a single value, it refers to the value calculated at 43–44% CO conversion after 100 h on stream.

3. Results and discussion

3.1. Support and catalyst characterization

3.1.1. Nitrogen adsorption/desorption

Fig. 1 shows the pore size distributions of the three Al_2O_3 supports. As shown in Table 1, the average pore diameters were 7, 12, and 27 nm. The other physical parameters were also different, the surface areas were 184, 186, and 114 m^2/g and the pore volumes 0.48, 0.73, and 0.86 cm^3/g. Impregnation, drying, and calcination reduced the surface area and pore volume similarly for all catalysts. For instance, the reduction in pore volume ranged from 32% to 38%. Deposition of metal precursor(s) did not have a strong impact on the average pore diameter of the samples. Furthermore, it did not influence the shape of the pore size distribution, but merely reduced the nitrogen uptake as shown in Fig. 1. In general, the variations in physical parameters of the supports are reflected in the properties of the final catalysts.

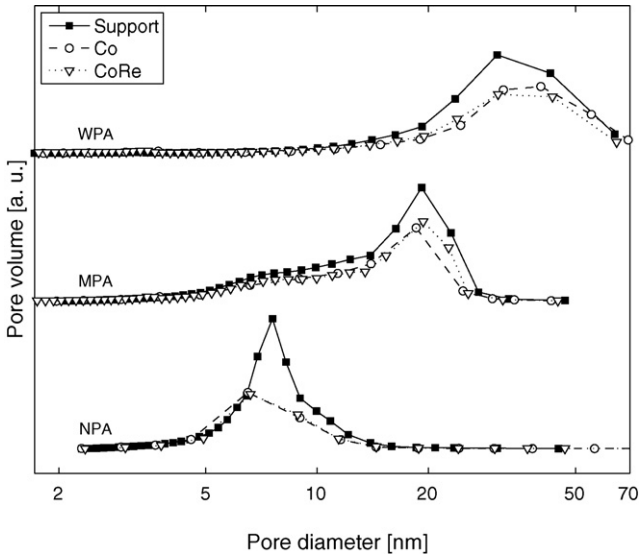

Fig. 1. Support and catalyst pore size distributions calculated from the nitrogen desorption branches using the Barrett–Joyner–Halenda method (filled symbol = support; open symbol = catalyst).

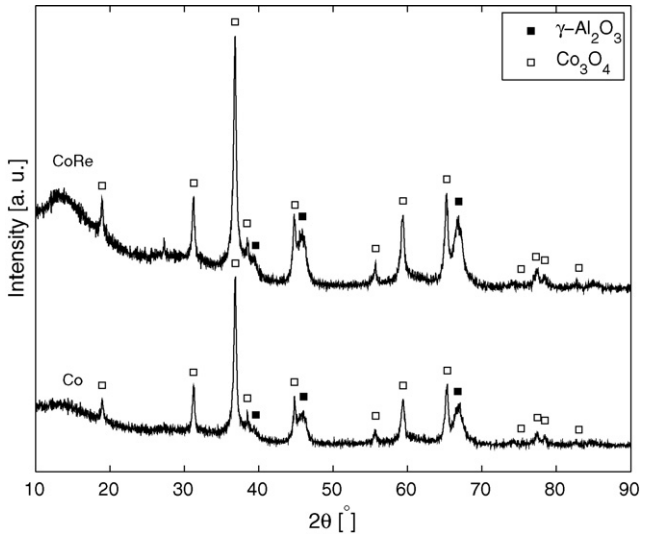

Fig. 2. X-ray diffraction patterns of catalysts Co/WPA, and CoRe/WPA.

3.1.2. X-ray diffraction

X-ray diffraction patterns of all supports confirmed the presence of only γ-Al_2O_3. In addition to γ-Al_2O_3, the impregnated samples exhibited reflections of Co_3O_4. Patterns are given for catalysts Co/WPA and CoRe/WPA in Fig. 2. The diffractograms of the two other pairs of catalysts showed exactly the same crystallographic reflections. As shown in Fig. 2, there was no difference for the un-promoted and Re-promoted sample. The Re loading of the promoted sample was too low to give detectable peaks. Since the catalysts did not show any other X-ray diffraction peaks, Co_3O_4 is the only detectable crystalline cobalt species present after catalyst calcination.

The only difference between the X-ray diffraction patterns of the calcined samples was the width of the Co_3O_4 peaks. For all catalysts, the Co_3O_4 crystallite size was calculated from the (3 1 1) reflection at $2\theta = 36.9^\circ$. The numbers are presented in Table 2. The relationship between the support pore diameter and the Co_3O_4 crystallite size is shown in Fig. 3. Two conclusions can be drawn. First, and most important, the Co_3O_4 crystallite size was controlled by the γ-Al_2O_3 support pore size. As shown in Fig. 3, we have previously found the same relationship for a large number of other γ-Al_2O_3 supports [9]. Second, the Co_3O_4 crystallites were slightly smaller for the promoted samples than for the un-promoted samples. Mauldin and Varnado [3] also observed that the presence of rhenium gives improved cobalt oxide dispersion. However, Storsæter et al. [6] reported largest Co_3O_4 crystallites for cobalt supported on narrow pore γ-Al_2O_3 and wide-pore TiO_2 when rhenium was present.

3.1.3. Temperature programmed reduction

Temperature programmed reduction profiles for all calcined samples are given in Fig. 4. The curves show three main reduction steps, centred between 500 and 540, 630 and 650, and 780 and 990 K. The first reduction step can be attributed to reduction of the residual cobalt nitrate remaining after calcination [9,18]. The last two reduction peaks can be assigned to a two-step reduction of Co_3O_4 to Co^0 via CoO as an intermediate species [19]. The catalysts showed no further peaks between 1203 and 1353 K. Thus, no cobalt aluminate or cobalt aluminate-like species were detected after impregnation, drying, and calcination.

As shown in Fig. 4, the peak attributed to reduction of Co_3O_4 to CoO was located in a narrow temperature region (630–650 K) for all six catalysts. Thus, the reducibility of supported Co_3O_4 did not depend on catalyst properties such as particle size, morphology, pore size, and surface area. The same conclusion was drawn by Castner et al. [20]. In contrast, the second step was largely dependent on catalyst properties. For both the un-promoted and promoted series of catalysts, the reduction area moved to slightly lower temperatures with increasing pore and particle size. Lower temperatures imply easier reduction and weaker metal–support interactions. These results are in agreement with Khodakov et al. [21] who observed that large particles are easier to reduce than small particles.

Fig. 4 also shows that rhenium significantly facilitated the reduction of CoO to Co^0. This is in agreement with Hilmen et al. [2] who suggested that metallic Re promotes reduction of cobalt oxide by hydrogen spillover. However, the role of Re as a reduction promoter was less pronounced at increasing pore and particle size. While introduction of Re decreased the reduction temperature by about 100 K for the narrow-pore catalyst, the reduction profiles of

Table 2
Characterization data. The experimental error ($\pm 2\sigma$) for the Co_3O_4 crystallite sizes calculated from X-ray diffraction is less than ±1 nm and is based on two independent runs for a selection of catalysts. The experimental error ($\pm 2\sigma$) for the cobalt metal dispersion is less than ±0.5% and ±2% for the degree of reduction.

Catalyst	Co_3O_4 crystallite size (nm)	Dispersion (%)	$d(Co^0)_{uncorrected}$ (nm)	Degree of reduction (%)	$d(Co^0)_{corrected}$ (nm)
Co/NPA	13.7	5.0	19.2	41	7.9
CoRe/NPA	12.0	8.7	11.1	63	6.9
Co/MPA	14.7	5.9	16.2	67	10.9
CoRe/MPA	14.6	7.9	12.2	74	9.1
Co/WPA	21.7	4.9	19.6	76	14.9
CoRe/WPA	21.1	6.5	14.9	76	11.4

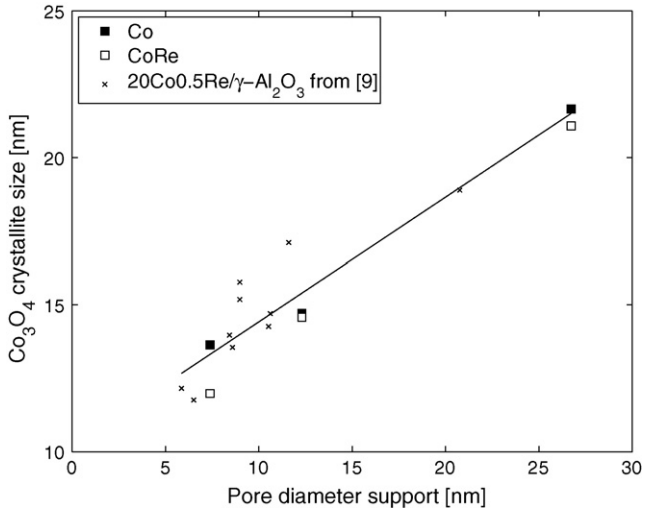

Fig. 3. Effect of the support pore diameter on the Co_3O_4 crystallite size calculated from X-ray diffraction data.

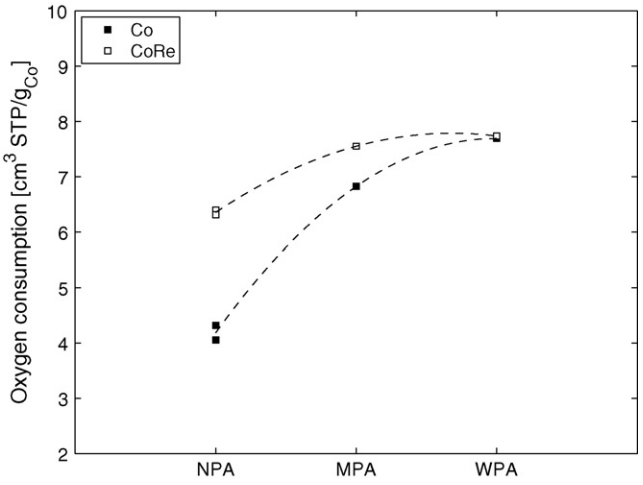

Fig. 5. Oxygen uptake during O_2 titration at 673 K.

the wide-pore-based catalysts were similar. The varying influence of Re of the different samples is probably related to the cobalt oxide crystallite size. The crystallites of catalyst Co/NPA are small and difficult to reduce. Re, therefore, has a large effect on the reducibility. For Co/WPA, the crystallites are large and relatively easy to reduce in the first place. Thus, Re does not exert a strong effect on the reducibility.

Temperature programmed reduction profiles were also recorded after normal reduction (623 K, 16 h). Only small amounts of hydrogen were consumed, indicating that the catalysts were almost completely reduced. However, the hydrogen consumption was greater for small crystallites than for large ones. Also, the hydrogen consumption was smaller when Re was present in the catalytic system.

3.1.4. Oxygen titration

Oxygen titration of the pre-reduced catalysts was done in order to determine the degree of reduction of the catalysts. The results are presented in Table 2 and illustrated in Fig. 5. The agreement between the oxygen titration data and the temperature programmed reduction profiles is excellent. As shown in Fig. 5, for the un-promoted series, the oxygen consumption increased strongly with increasing pore and particle size. The reduction profiles in Fig. 4 also showed that the CoO to Co^0 peak was shifted significantly to lower temperatures as the pore and particle size increased. For the series of promoted catalysts, the increase in oxygen uptake with increasing pore and particle size was more moderate. The difference in reduction profiles of the promoted catalysts was also smaller. Finally, the two catalysts supported on wide-pore alumina showed very similar reduction profiles and practically identical oxygen uptake.

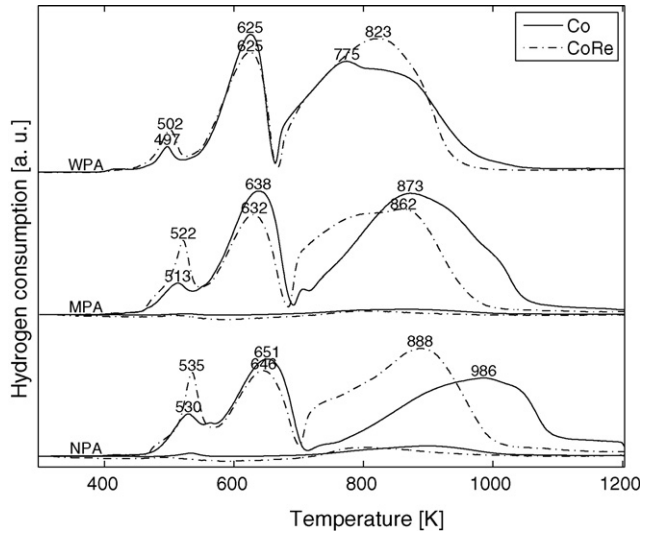

Fig. 4. Temperature programmed reduction profiles of calcined catalysts.

3.1.5. Hydrogen chemisorption

Chemisorption of hydrogen on the reduced samples was used to measure cobalt dispersion and, in combination with oxygen titration, to estimate the cobalt particle size. As shown in Table 2, the cobalt dispersion of the Re-promoted catalysts was higher than the dispersion of the un-promoted counterparts. However, the gain in cobalt dispersion upon Re addition was largely depending on the physical parameters of the catalysts. While introduction of Re increased the cobalt dispersion significantly for the narrow-pore catalyst (74%), the increase was smaller for the two other catalysts (34% and 33%). This is consistent with Figs. 4 and 5 which showed that the influence of Re with respect to reducibility was largest for cobalt supported on narrow-pore alumina. As already mentioned, the favourable impact of Re can be explained by spillover of hydrogen from rhenium to cobalt oxide.

3.1.6. X-ray absorption spectroscopy

XANES spectra were recorded for two catalysts (Co/NPA and CoRe/NPA) during *in situ* reduction. These were compared with reference spectra of Co_3O_4, CoO, and a Co^0 foil. In agreement with our recent investigation [19], Co_3O_4 was reduced in two steps to Co^0 with CoO as intermediate. The first reduction step took place at 623 K for both catalysts. This temperature correlates well with the temperatures observed for the same samples in standard temperature programmed reduction (646 and 651 K). However, note that the heating ramp rate and the concentration of hydrogen in the gas mixture were different for the two reduction experiments. Thus, the reduction temperatures will vary.

The further reduction was very different for the two samples. In agreement with TPR and O_2 titration data, the degree of reduction was significantly higher for catalyst CoRe/NPA than for catalyst Co/NPA. After 3.5 h of reduction, the degree of reduction of these samples was 70% and 22%, respectively. It should also be mentioned that the degree of reduction did not change when

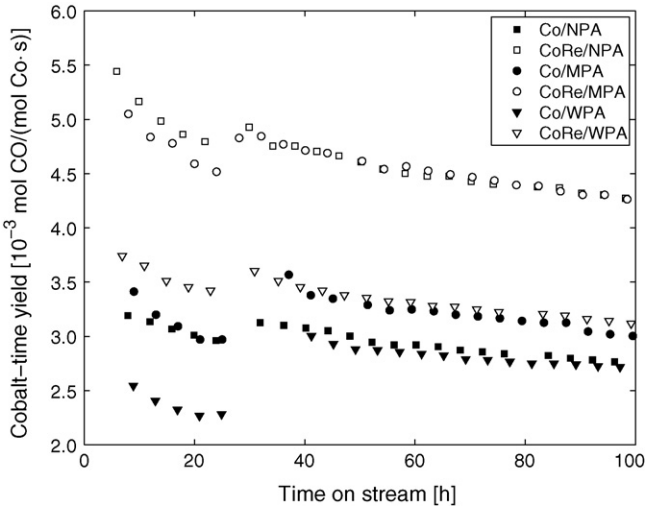

Fig. 6. Cobalt-time yields measured at T = 483 K, P = 20 bar, and H_2/CO = 2.0.

the catalyst was exposed to synthesis gas. Thus, no oxidation occurred at the applied experimental conditions. However, note that the CO conversion and, accordingly, the water partial pressure were not measured during the course of the reaction.

3.2. Fischer–Tropsch synthesis

Since the performance of supported cobalt Fischer–Tropsch catalysts is very sensitive to reaction conditions and reactant conversion, care was taken in order to ensure that all the catalysts were subjected to exactly the same reactor-setup and gaseous environment during synthesis.

3.2.1. Activity

Cobalt-time yields are presented in Fig. 6. In addition, cobalt and site-time yields recorded after 8–12 h on stream are given in Table 3. Although the initial cobalt-time yields varied substantially (3.1–6.7 $\times$ 10^{-3} mol CO/(mol(Co) s)), the site-time yields were, within experimental error, constant (51–64 $\times$ 10^{-3} s^{-1}). Accordingly, Re does not modify the site-time yield and the activity can directly be predicted from the number of cobalt atoms on the surface. The same conclusion was drawn by Mauldin and Varnado [3]. The site-time yields are also close to the ones obtained by Storsæter et al. [6] who ran Fischer–Tropsch synthesis at the same conditions for cobalt supported on γ-Al_2O_3, SiO_2, and TiO_2. It should be mentioned that Bezemer et al. [22] found cobalt particles smaller than 8 nm in size to be less active than larger particles. No such difference was found in this investigation. However, note that only one catalyst had an average particle size below 8 nm in size (CoRe/NPA) and that the calculated particle size is dependent on the H_2 chemisorption and O_2 pulse titration measurement conditions. Also, the cobalt particle size distribution is unknown. Thus, there are not sufficient data to draw any conclusions about a possible particle size effect on the cobalt intrinsic activity. Finally, it should be emphasised that the difference in cobalt-time yield was largest for the narrow-pore catalysts and smallest for the wide-pore catalysts. In fact, while the steady-state activity (*i.e.* after 100 h on stream) of catalyst CoRe/WPA was only 15% higher than the activity of catalyst Co/WPA, the corresponding difference between the NPA-based catalysts was larger than 50%. These variations can be explained by the varying influence of Re for the different catalysts as described earlier.

Table 3
Cobalt-time yields and site-time yields calculated after 8–12 h on stream (T = 483 K, P = 20 bar, H_2/CO = 2.0, and GHSV = 15 N l/(g_{cat} h)). The experimental error ($\pm 2\sigma$) for the site-time yield is $\pm 10 \times 10^{-3}$ s^{-1}.

Catalyst	Cobalt-time yield ($\times 10^3$ mol CO/(mol(Co) s))	Site-time yield ($\times 10^3$ s^{-1})
Co/NPA	3.9	51
CoRe/NPA	6.7	63
Co/MPA	4.2	54
CoRe/MPA	6.2	64
Co/WPA	3.1	52
CoRe/WPA	4.6	58

As shown in Fig. 6, the deactivation rates from 0 to 24 h were higher for the most active catalysts (*e.g.* the ones giving highest cobalt-time yield and CO conversion). Thus, higher CO conversion apparently leads to more rapid deactivation as also seen by others [4]. The deactivation rates (and the CO conversion) were similar for all samples from 24 to 100 h although some of the catalysts contained Re. Also, there were large variations in cobalt particle size. These results add further speculations as to which factors are causing deactivation of cobalt Fischer–Tropsch catalysts. While oxidation of cobalt has been postulated as a deactivation mechanism [23], Saib et al. [24] recently ruled out this possibility for cobalt particles larger or equal to 6 nm in diameter. Finally, it must be mentioned that 100 h on stream in a fixed-bed reactor are probably not sufficient to make a trustworthy distinction between the deactivation rates of the different catalysts.

3.2.2. Selectivity

Although often neglected in literature, it is necessary to compare the product selectivity of different catalysts at the same CO conversion level and, therefore, at the same H_2O partial pressure. It is well known that the H_2O concentration level is important for the C_{5+} selectivity [25,26]. As shown in Fig. 7, the conversion level was almost identical for all the catalysts giving reliable comparison between the catalysts.

As shown in Fig. 8, the C_{5+} selectivity strongly increased with increasing pore diameter for both series of catalysts. Table 4 shows that both a lower CH_4 and C_2–C_4 selectivity contributed to the improved C_{5+} selectivity. Thus, the chain-growth probability, often denoted α, increased with increasing pore diameter. We have previously shown the same trend for 10 other catalysts [9]. It has been proposed that the difference in selectivity observed for cobalt on different supports can be related to the extent of α-olefin re-adsorption [27–29]. However, since the olefin/paraffin ratios of all catalysts were very similar (Table 4), it is not likely that re-

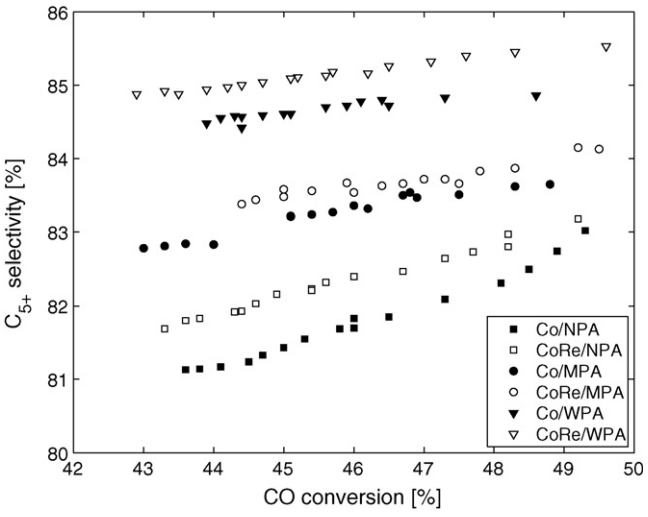

Fig. 7. C_{5+} selectivity measured at T = 483 K, P = 20 bar, and H_2/CO = 2.0.

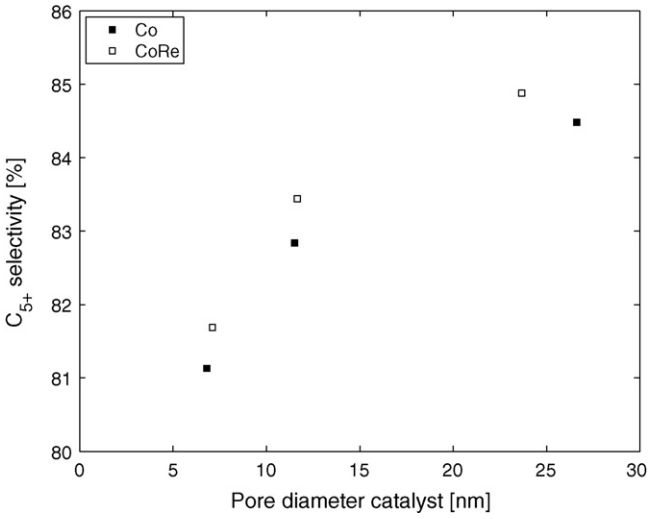

Fig. 8. Effect of pore diameter on the C_{5+} selectivity at T = 483 K, P = 20 bar, H_2/CO = 2.0, and 43–44% CO conversion.

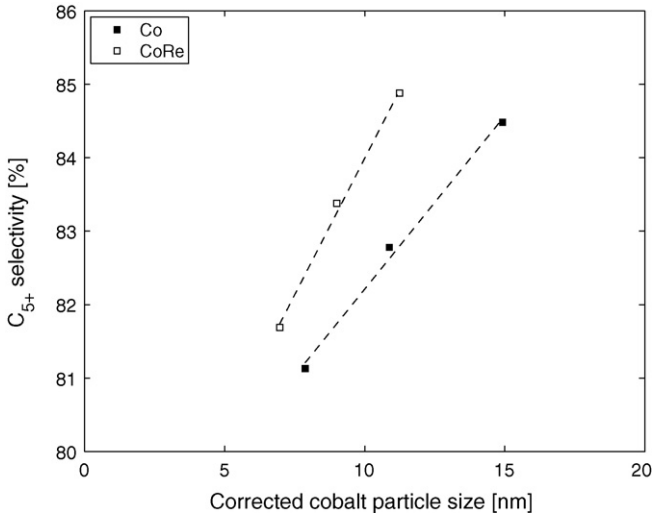

Fig. 9. Effect of cobalt particle size on the C_{5+} selectivity at T = 483 K, P = 20 bar, H_2/CO = 2.0, and 43–44% CO conversion.

Table 4
Selectivity data at T = 483 K, P = 20 bar, H_2/CO = 2.0, and 43–44% CO conversion. The experimental error ($\pm 2\sigma$) for the C_{5+} selectivity is ±0.6%.

Catalyst	Hydrocarbon selectivity (%)			Olefin/paraffin ratios				
	C_1	C_2–C_4	C_{5+}	$C_{2=}/C_{2-}$	$C_{3=}/C_{3-}$	$C_{4=}/C_{4-}$	$C_{5=}/C_{5-}$	$C_{6=}/C_{6-}$
Co/NPA	9.0	9.9	81.1	0.12	2.4	1.5	1.2	0.85
CoRe/NPA	8.8	9.5	81.7	0.12	2.4	1.5	1.2	0.83
Co/MPA	8.6	8.7	82.8	0.10	2.1	1.2	0.95	0.63
CoRe/MPA	8.4	8.3	83.4	0.10	2.3	1.4	1.1	0.74
Co/WPA	8.0	7.5	84.5	0.08	2.1	1.2	0.92	0.59
CoRe/WPA	8.0	7.2	84.9	0.08	2.3	1.4	1.1	0.74

C_{i-} = paraffin selectivity of carbon number i. $C_{i=}$ = olefin selectivity of carbon number i.

adsorption can explain the variations in selectivity between the narrow-pore catalysts and the wide-pore catalysts. This is consistent with investigations by Shi and Davis [30] and Rytter et al. [31].

The C_{5+} selectivity of the Re-promoted samples was higher than the selectivity of the corresponding un-promoted catalysts. Also, the results in Table 4 indicate that Re increases the chain-growth probability since both the selectivity to CH_4 and C_2–C_4 decreased. The results are in agreement with Schanke et al. [7] who found slightly higher selectivity for cobalt supported on γ-Al_2O_3 in presence of Re than in absence of Re. In contrast, Bertole et al. [5] concluded from steady-state isotopic transient kinetics analysis that Re at a Re/Co weight ratio of 0.1 does not influence the Fischer–Tropsch selectivity. However, note that the investigation of Bertole et al. [5] was done at different conditions, *i.e.* 494 K and 6.5 bar.

Fig. 9 shows that the C_{5+} selectivity cannot only be correlated to the pore diameter, but also to the cobalt particle size. For both the un-promoted and promoted series of catalysts, a correlation coefficient close to 1 was obtained. Since the variations in selectivity cannot be explained entirely by diffusion effects (*e.g.* different extents of olefin re-adsorption), it is suggested that the C_{5+} selectivity is related to the cobalt particle sizes rather than pore diameter. In fact, Rytter et al. [31] have concluded that diffusion is pore size independent. As shown in Fig. 9, the Re samples exhibited higher selectivity than the un-promoted catalysts at a similar particle size. Thus, Re probably changes the termination probability of the growing hydrocarbon chain through a chemical effect. Bezemer et al. [22] also found the particle size to impact the C_{5+} selectivity, but only for particles between 3 and 8 nm in size. It should, however, be mentioned that their investigation included few data points at Fischer–Tropsch conditions and that the C_{5+} selectivity was measured at different CO conversions (13–84%). Nevertheless, the results in Fig. 9 indicate that their results can be extended to larger particles. However, we speculate that the cobalt particle size is not the only parameter that influences the C_{5+} selectivity. In fact, Rytter et al. [31] observed significantly higher selectivity for cobalt supported on α-Al_2O_3 than for cobalt supported on γ-Al_2O_3 although the average particle size on all these catalysts was larger than the limit set by Bezemer et al. [22], namely 8 nm. Thus, the support must play an important role in determining the C_{5+} selectivity.

4. Conclusions

A systematic study of the effect of rhenium for γ-Al_2O_3 supported cobalt catalysts has been carried out. Re influences the catalyst and the catalytic performance in several ways. Re increases the reducibility of cobalt supported on γ-Al_2O_3. Re also increases the cobalt dispersion and, therefore, the Fischer–Tropsch synthesis activity. The C_{5+} selectivity is also increased when Re is incorporated into the catalyst. The magnitude of the positive impact is, however, dependent on the catalyst system. While Re has a great impact on the catalytic performance of the narrow pore-based catalysts, the effect is smaller for the wide-pore-based catalysts. No significant variations in deactivation rates were found between the catalysts up to 100 h on stream.

Acknowledgements

The financial support from the Norwegian Research Council through the KOSK programme is greatly acknowledged. The authors also thank Statoil ASA for financial support and for supplying alumina samples. The project team at the Swiss-Norwegian Beamlines at ESRF is greatly acknowledged for experimental assistance.

References

[1] C.H. Mauldin, United States Patent 4,568,663 (1986), to Exxon Research and Engineering Co.

[2] A.M. Hilmen, D. Schanke, A. Holmen, Catal. Lett. 38 (1996) 143.
[3] C.H. Mauldin, D.E. Varnado, Stud. Surf. Sci. Catal. 136 (2001) 417.
[4] T.K. Das, G. Jacobs, P.M. Patterson, W.A. Conner, J. Li, B.H. Davis, Fuel 82 (2003) 805.
[5] C.J. Bertole, C.A. Mims, G. Kiss, J. Catal. 221 (2004) 191.
[6] S. Storsæter, Ø. Borg, E.A. Blekkan, A. Holmen, J. Catal. 231 (2005) 405.
[7] D. Schanke, S. Eri, E. Rytter, C. Aaserud, A.-M. Hilmen, O.A. Lindvåg, E. Bergene, A. Holmen, Stud. Surf. Sci. Catal. 147 (2004) 301.
[8] E. Rytter, S. Eri, International Publication Number WO 2006/010936 A1 (2006), to Statoil ASA and PetroSA.
[9] Ø. Borg, S. Eri, E.A. Blekkan, S. Storsæter, H. Wigum, E. Rytter, A. Holmen, J. Catal. 248 (2007) 89.
[10] S. Brunauer, P.H. Emmett, E. Teller, J. Am. Chem. Soc. 60 (1938) 309.
[11] E.P. Barrett, L.G. Joyner, P.P. Halenda, J. Am. Chem. Soc. 73 (1951) 373.
[12] P. Scherrer, Göttingen Nachrichten 2 (1918) 98.
[13] E.A. Blekkan, A. Holmen, S. Vada, Acta Chem. Scand. 47 (1993) 275.
[14] R.C. Reuel, C.H. Bartholomew, J. Catal. 85 (1984) 63.
[15] R.D. Jones, C.H. Bartholomew, Appl. Catal. 39 (1988) 77.
[16] T. Ressler, J. Synchrotron. Rad. 5 (1998) 118.
[17] T. Ressler, J. Wong, J. Roos, I.L. Smith, Environ. Sci. Technol. 34 (2000) 950.
[18] A. Lapidus, A. Krylova, V. Kazanskii, V. Borovkov, A. Zaitsev, J. Rathousky, A. Zukal, M. Jančálková, Appl. Catal. 73 (1991) 65.
[19] Ø. Borg, M. Rønning, S. Storsæter, W. van Beek, A. Holmen, Stud. Surf. Sci. Catal. 163 (2007) 255.
[20] D.G. Castner, P.R. Watson, I.Y. Chan, J. Phys. Chem. 94 (1990) 819.
[21] A.Y. Khodakov, J. Lynch, D. Bazin, B. Rebours, N. Zanier, B. Moisson, P. Chaumette, J. Catal. 168 (1997) 16.
[22] G.L. Bezemer, J.H. Bitter, H.P.C.E. Kuipers, H. Oosterbeek, J.E. Holewijn, X. Xu, F. Kapteijn, A.J. van Dillen, K.P. de Jong, J. Am. Chem. Soc. 128 (2006) 3956.
[23] A.M. Hilmen, D. Schanke, K.F. Hanssen, A. Holmen, Appl. Catal. A 186 (1999) 169.
[24] A.M. Saib, A. Borgna, J. van de Loosdrecht, P.J. van Berge, J.W. Niemantsverdriet, Appl. Catal. A 312 (2006) 12.
[25] J.K. Minderhoud, M.F.M. Post, S.T. Sie, E.J.R. Sudholter, United States Patent 4,628,133 (1986), to Shell Oil Company.
[26] E.A. Blekkan, Ø. Borg, V. Frøseth, E. Rytter, Royal society of chemistry, Catalysis 20 (2007) 13.
[27] E. Iglesia, S.L. Soled, R.A. Fiato, J. Catal. 137 (1992) 212.
[28] E. Iglesia, S.C. Reyes, R.J. Madon, S.L. Soled, Adv. Catal. 39 (1993) 221.
[29] E. Iglesia, S.L. Soled, R.A. Fiato, G.H. Via, Stud. Surf. Sci. Catal. 81 (1994) 433.
[30] B. Shi, B.H. Davis, Catal. Today 106 (2005) 129.
[31] E. Rytter, S. Eri, T.H. Skagseth, D. Schanke, E. Bergene, R. Myrstad, A. Lindvåg, Ind. Eng. Chem. Res. 46 (2007) 9032.